phys. stat. sol. (c) **0**, No. 6, 1835–1845 (2003) / **DOI** 10.1002/pssc.200303137

The origin of the PL photoluminescence Stokes shift in ternary group-III nitrides: field effects and localization

M. Strassburg[1], **A. Hoffmann**[*, 1], **J. Holst**[1], **J. Christen**[2], **T. Riemann**[2], **F. Bertram**[2], and **P. Fischer**[2]

[1] Institut für Festkörperphysik, Technische Universität Berlin, Hardenbergstr. 36, 10623 Berlin, Germany
[2] Institut für Experimentelle Physik, Otto-von-Guericke Universität Magdeburg,Universitätsplatz 2, 39106 Magdeburg, Germany

Received 4 March 2003, revised 4 August 2003, accepted 4 August 2003
Published online 28 August 2003

PACS 78.20.Hp, 78.30.Fs, 78.45.+h, 78.47.+p, 78.67.De, 78.67.Hc

We report on a systematic analysis of the localization and separation mechanisms of carriers and their co-existence in ternary group-III nitrides. AlGaN/GaN and InGaN/GaN multi-quantum-well (MQW) structures grown on sapphire substrate were investigated. Although the localization and separation mechanisms of carriers result in a similar behavior of the luminescence properties (e.g. both lead to blue shift of emission energy with increasing excitation density and vice versa a transient red shift after pulsed excitation), a clear distinction between these mechanisms is given by optical investigations with resonant and non-resonant excitation. Carrier separation due to a localization induced by internal electric fields described by the quantum-confined Stark-effect exist in all MQW structures and was found to be important in particular in the AlGaN/GaN MQWs. In general, the internal electric fields lead to a reduction of the luminescence efficiency. A fundamental localization mechanism, i.e. the localization in nm-scale islands of local minimum energy directly result from the spatial energy fluctuations due to disorder (e.g. alloy or QW thickness fluctuations). Especially at temperatures below 100 K, this mechanism dominates the carrier localization in the InGaN/GaN system. Evidence is given by the unique S-shape temperature dependence of peak energy and the existence of a mobility edge. Due to the localization of carriers in nm-scaled islands the overlap of its wavefunctions increases, which strongly increases the efficiency of the light output. This effect is significant weaker but still detectable in the AlGaN/GaN system.

1 Introduction

The mechanism of the optical recombination in low-dimensional InGaN and AlGaN quantum structures has been under controversial discussion in recent years [1]. The observed red shift in luminescence and absorption experiments was assigned to spontaneous and strain-induced piezo-electric fields [2] as well as localization effects in islands formed by segregation during the growth of ternary alloys [3]. In the present paper we give an overview of the field effects and the localization properties in ternary group-III-nitride structures of reduced dimensionality. We will show that a similar experimental effect (red shift of luminescence) is caused by two principle different mechanisms. On the one hand, strong electric fields amplify the localization of carriers at the opposite interfaces of the quantum well system and thus, lead to a separation of electrons and holes. Otherwise, quantum dot-like structures provide localization of charge carriers and excitons. Here, the overlap of the electron and hole wavefunctions and therefore the PL efficiency may increase. The localization mechanisms in ternary group-III nitrides will be analyzed, distinguished and assigned to material systems and structural particularities.

[*] Corresponding author: e-mail: hoffmann@physik.tu-berlin.de, Phone: +49 30 314 22001, Fax: +49 30 314 22064

2 Experimental

To study the impact of internal electric fields AlGaN/GaN multiple-quantum wells (MQWs) were investigated. This material system was chosen, because the carriers are localized in the binary compound (GaN). Hence, no alloy broadening is to consider for the localization of carriers as it is typically for ternary compounds accept the neglectable weak effect of alloy fluctuations in the AlGaN barriers. A series of AlGaN/GaN MQWs with a variation of the GaN QW width from 2.2 to 4.5 nm were investigated. The samples were grown by MOCVD consisting of a threefold GaN/AlGaN MQW embedded in AlGaN claddings. To achieve a lattice-matched structure, the aluminum content in the MQWs was chosen to 20-30%, whereas the Al content in the ternary claddings is 10 %. The lower cladding was grown on a GaN buffer on sapphire substrate.

A further AlGaN/GaN sample was grown by MOCVD. It differs from the series described above by the MQW system consisting of a tenfold stack of 3 nm thick GaN layers separated by 20 nm thick AlGaN barriers. This sample was applied for gain measurements and investigations at high-excitation densities.

Additionally, for the pump-and-probe experiments a specially designed sample was grown by MBE. This sample consists of a tenfold $Al_{0.11}Ga_{0.89}N$/GaN MWQ. The thickness of the GaN is 1.5 nm and of the AlGaN barriers 5 nm. The MQW system is embedded in AlGaN claddings of several 100 nm thicknesses.

A series of (InGaN/GaN MQWs) samples was chosen to investigate the impact of potential fluctuations. Sample A belongs to a series of MBE-grown samples on sapphire, with an 18 µm GaN (MOVPE) layer and capped by a 30 nm GaN layer. The optical active region of sample A consists of a tenfold 5 nm InGaN MQW with 4 nm GaN barriers. The indium concentration of 6.7 % was determined by XRD. Sample B is also an tenfold InGaN/GaN MQW with a thickness of 4 nm each, grown with different growth temperatures for the QWs and the barriers by low-pressure MOCVD on ~2 µm GaN buffer layer on c-sapphire substrates in a horizontal production-type reactor AIX 2600 G3 in 2000 HT configuration. The In composition was measured by XRD to be 12.5 % with a GaN barrier thickness of 7.7 nm. The GaN buffer layer was grown at 1180 °C. The growth temperatures of the InGaN QWs and the GaN barriers were 750 °C and 950 °C, respectively. For a more detailed description see Ref. [4].

Photoluminescence (PL) was excited by the 325 nm line of a HeCd-laser. The samples were mounted in a cryostat allowing the variation of temperatures between 2 K and 300 K. The spectral resolution of the detection system was better than 0.2 meV. The high-excitation density investigations were performed using a dye laser pumped by an Excimer-laser providing pulses with a duration of 15 ns at a repetition rate of 30 to 50 Hz and a total energy of up to 20 µJ. For the pump-and-probe spectroscopy (PPS) the Excimer- laser emission was used for the pump beam while for the probe a dye laser was applied. The gain measurements were performed using the variable stripe-length method [5]. The experimental set up for the spectrally-, spatially-, and time-resolved cathodoluminescence experiments is described elsewhere [6,7].

3 Results and discussion

Carrier localization and separation in ternary InGaN- and AlGaN-based heterostructures is reported by many authors and was found to determine the optical properties [1-3]. Two different mechanisms were found. Both, the quantum-confined Stark-effect (QCSE) and the localization in quantum dot (QD)-like structures having similar effect on the emission wavelength namely causing a pronounced blue shift of PL maximum with increasing excitation density in the active region of UV, blue or green emitting devices. The QCSE is caused by internal electric fields and is attributed to govern the optical properties of AlGaN-based devices. Also in the case of InGaN the presence of strong piezoelectric fields is demonstrated [8,9]. Furthermore, some authors explain the recombination behavior solely by the QCSE [10]. In the following we will show, that the localization in QD-like island structures must not be neglected to understand the optical recombination in group-III nitride heterostructures.

3.1 Influence of internal electric fields

To study the influence of the electric fields and to avoid perturbations of the observed effects by localization in potential fluctuations the AlGaN/GaN system was chosen. Due to the Coulomb interaction between electron and holes, excitons are formed. These excitons having a Bohr radius of several nm. Therefore, internal electric fields may separate the electron and the hole of an exciton to each heterointerfaces of a quantum well. The main advantage of this GaN/AlGaN heterosystem is the confinement of the excitons in the binary GaN QW. Hence the localized 2D excitons only very weakly experience the residual alloy fluctuations in the AlGaN due to a partial tunneling into the MQW barriers. Nevertheless, a pronounced blue shift of the luminescence peak position is usually observed with increasing excitation density [11]. In the following it will be demonstrated that the emission is governed by spontaneous polarization and piezo-electric fields. As it will be shown later, a good agreement between theoretical predictions and experimental results were achieved. The separation of carriers (i.e., electrons and holes of excitons) in QW due to electric fields is described by the quantum-confined Stark-effect (QCSE). The carriers with opposite charge are located at different interfaces of the well and thus the overlap of their wavefunctions reduces. This strongly influences the opto-electronic properties of the heterostructures.
The main parameters determining the emission properties are the exact alignment of the polarization, the thickness of the quantum well and the Al-content of the barriers.
To illustrate the effect of inner electric fields AlGaN/GaN MQW structures differing in the well and barrier thickness were investigated. The polarization in these samples P_{total} can be written as

$$P_{total} = P_{TS} + P_{mis} + P_{spont} = P_{piezo} + P_{spont}\,, \tag{1}$$

where P_{TS} is the polarization caused by the thermal strain and P_{mis} is the polarization due to the lattice mismatch. In dependence of the barrier (L_B) and the well thickness (L_W) the total field can be obtained after [12] by

$$F_w = \frac{L_B\left(P^B_{total} - P^W_{total}\right)}{\varepsilon_0\left(L_B\varepsilon_W + L_W\varepsilon_B\right)}. \tag{2}$$

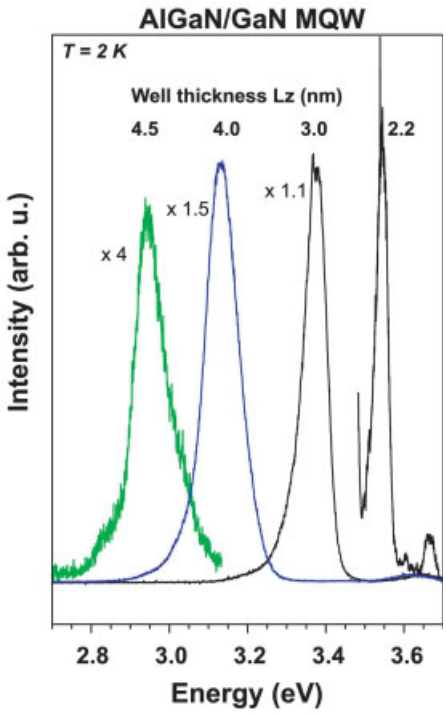

Fig. 1 (online colour at: www.interscience.wiley.com) Photoluminescence (PL) spectra of AlGaN/GaN MQW structures at low temperatures. The varied parameter is the well thickness marked at the respective PL spectra.

The internal electric field strongly influences the emission energy as shown in Fig. 1. The emission energy shifts to lower energies with increasing well thickness. For well thickness above 2.5 nm the emission energy is lower than the GaN bandgap. Obviously, the internal electric fields overcompensates the confinement effect, which causes a blue shift of the emission energy. Furthermore, this QCSE results in reduction of transition probability explaining the observed decrease in PL intensity for thicker wells. The broadening of the PL linewidth is attributed particularly to thickness fluctuations in the AlGaN/GaN MQWs.

Another effect of the QCSE on the emission is the reduction of the transition probability. The internal electric fields limit the optical recombination due to the reduction or break-up of the overlap of electron- and hole-wavefunctions. Thus, the recombination probability is dramatically reduced. Hence, a steep increase of the lasing threshold is observed. Especially in structures with elevated Al content in the barriers, this tendency is pronounced. Their impact on the optical properties are exemplarily illustrated by high-excitation investigations of the MOCVD-grown tenfold AlGaN/GaN MWQ.

In Figure 2 a comparison of low-excitation and high-excitation PL (stimulated emission) is depicted. At low excitation energies the PL is dominated by QW luminescence around 3.4 eV. A second emission band at 3.52 eV is attributed to a spatially direct transition into the GaN well. With increasing excitation energy by a factor of 100 a pronounced blue shift of the QW luminescence is observed with a maximum at 3.51 eV. Above a threshold of 100 $kWcm^{-2}$ lasing is detected at this wavelength. This behavior is confirmed by gain spectroscopy revealing optical amplification in the same spectral range. Lasing and optical gain is detected 120 meV above the QW luminescence energy demonstrating the strong screening of the QCSE at elevated excitation densities. Theoretical approximations [12] deliver 10 to 20 $kWcm^{-2}$ per well being in good agreement with the experimentally obtained results presented here. The results underline that the strength of the electric fields is extraordinarily important for the recombination probability and hence for the radiative recombination.

Although the internal electric fields may mainly contribute to the separation of electron and holes, the presence of thickness fluctuations of the GaN QWs can not completely excluded. Since the excitons are localized in the QW areas with larger (thinner) thickness, the separation of carriers increases (decreases) due to their localization at opposite heterointerfaces. Thus the QCSE is to expect larger (smaller) than the

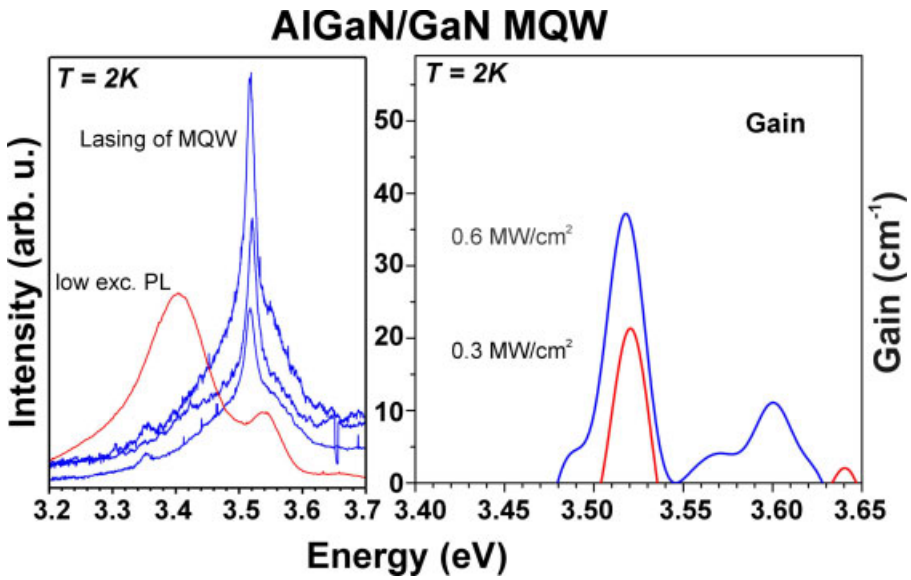

Fig. 2 (online colour at: www.interscience.wiley.com) Comparison of photoluminescence and stimulated emission (left) and gain (right) of a tenfold AlGaN/GaN MQW structure. Gain around 3.6 eV is generated in the 300 nm thick AlGaN cap layer.

average value for a given QW thickness. However, more precise information of the recombination and amplification processes is given by the PPS. The PPS allows a direct observation of the distribution and the recombination channels. Furthermore, the line widths of the emission bands are reduced by the resonant excitation. Figure 3 shows PP spectra of the MBE-grown GaN/AlGaN MQW sample. The excitation densities were varied from 10 kWcm^{-2} to 1 MWcm^{-2}. At the lowest excitation density, a bleaching of absorption is detected around 3.48 eV, while with increasing excitation densities this absorption (gain) structure vanishes. This structure is assigned to the emission of GaN. The observed bleaching is caused by the generation of optical gain. Due to the spectral position and former investigations [13] the gain is attributed to radiative decay of biexcitons.

The most striking feature is a strong induced absorption at 3.65 eV. With increasing excitation density this absorption becomes weaker and its maximum shifts to lower energies. The origin of the absorption is the quantized exciton in the MQW. The decrease of induced absorption (with increasing excitation density) shows the saturation of the excitonic recombination. This behavior is attributed to the rising screening of the Coulomb interaction resulting in a reduction of the excitonic binding energy and thus in a renormalization.

Additionally, an absorption bleaching was observed at 3.56 eV. The maximum of this structure shows a blue shift at elevated excitation densities and is located at 3.59 eV at 1 MWcm^{-2}. This structure is assigned to excitons localized in thickness fluctuations of the MQW [14]. The blue shift is explained by successive filling of localized states with increasing excitation density.

Localized excitons generate optical amplification (gain) meanwhile an induced absorption is observed for the electron and hole states in the MQW. The gain threshold density of excitons localized in fluctuations is by far smaller than that of the excitons localized in the MQW by the internal electric field. The latter amounts to 450 kVcm^{-1} for the active GaN QW layers. The excitons being not localized in fluctua-

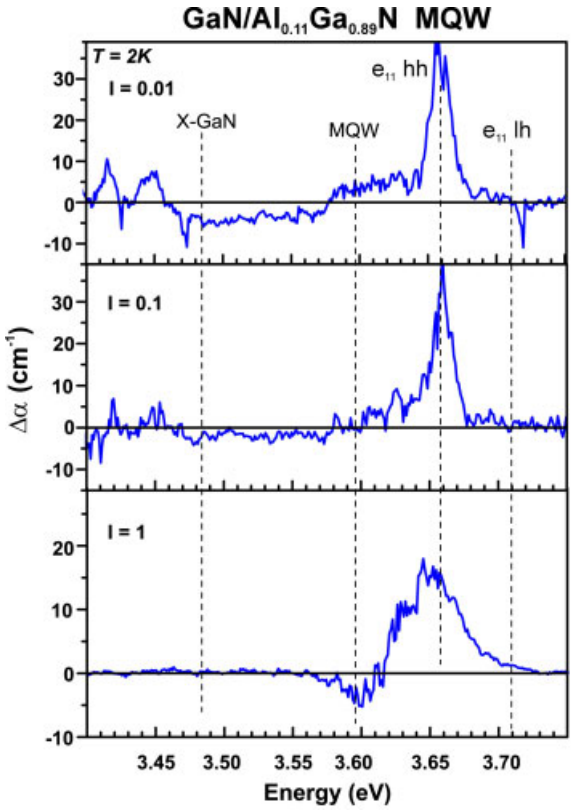

Fig. 3 (online colour at: www.interscience.wiley.com) Derivation of the absorption of the probe signal recorded by pump-and-probe spectroscopy for a 10fold GaN/AlGaN MQW at 2 K. The excitation density of the probe beam was varied from 10 kWcm^{-2} to 1 MWcm^{-2}.

tion potentials contribute to optical gain when the internal electric field is screened. Again, the role of localization and separation of carriers is demonstrated.

As it was mentioned above, to understand the emission properties of GaN/AlGaN structures the quantum-confined Stark-effect has to be included. All luminescence properties are strongly influenced by the presence of internal electric fields. The overlap of electron- and hole-wavefunctions is reduced due to its separation (localization at each side of the heterointerfaces). Therefore, the emission probability decreases lowering e.g. the efficiency of opto-electronic devices. Furthermore, due to the electric fields the exciton binding energy is reduced by a factor of 2-3 [12,15]. This is important so far as the application of excitonic devices is desirable, since high thermal stability and low threshold densities are the main advantages of such devices.

In order to compensate the internal electric fields, an enhanced effort on the sample design (e.g., appropriate quaternary compounds) is necessary to avoid the separation of electrons and holes to each side of the heterointerface. Theoretical investigations predict field free AlInGaN/GaN heterostructures [8,16,17], when the spontaneous polarization is compensated by perfectly matched strain induced piezoelectric fields. Also the reconstruction of the hetero-interface may contribute to the internal electric field as it was theoretically shown by Smith et al. [18].

Exciton localization and carrier separation in group-III nitrides has become a very prosperous field of investigation since it determines the opto-electronic properties of heterostructure devices. It was shown that separation of carriers due to internal electric fields reduces the efficiency of luminescence processes. In the next chapter we report on 3D carrier localization in nm-scaled potential islands.

3.2 Localization in randomly distributed potential fluctuations

The localization mechanism presented in this chapter strongly differs from that described above. Although a blue shift may be detected with increasing excitation densities in PL experiments, there are no further similarities to the behavior of carriers affected by electric fields. Especially, the origin of this behavior differs strongly, because the electrons and holes are localized in islands. Hence, the spatial overlap of their wavefunctions is increased. The InGaN/GaN heterosystem can be seen as a model system for the investigation of carrier and exciton localization in potential fluctuations generated by statistical distribution of local energy. In has a solubility limit in GaN and tends to segregate in the ternary InGaN. Thereby, the growth of homogeneous QWs is prevented and the formation of islands occurs.

More generally speaking, the formation of a ternary compound by epitaxial growth in principle results in chemical disorder leading to more or less pronounced spatial variation of the alloy composition on a microscopic scale. Such material fluctuations are widely studied in different III-V compounds and wide bandgap II-VI compounds [19]. Their size usually ranges from a few nm to several tens of nm. Thus they may act as quantum dots (QDs) providing a 3D localization for excitons and/or single carriers. The localization of carriers and/or excitons in these potential minima strongly influences the optical emission. More over it is found to be responsible for the high efficiency of light generation in InGaN-based LEDs and LDs [20]. Structural investigations by high-resolution TEM indeed revealed dense arrays of InN-rich nano-domains having a size of 3-5 nm and a density of 10^{11} to 10^{12} cm^{-2} [19,21,22]. However, the formation of these QD-like islands strongly depends on the growth conditions [23].

In this chapter evidence of exciton localization in such QD-like structures will be presented. The localization determines either the relaxation dynamics or the optical gain. Degushi et al. [24] have firstly shown that the segregation process in InGaN structures directly influence the lasing processes. Below it will be demonstrated that the localization in QD-like structures has to taken into account to understand the recombination behavior in ternary InGaN heterostructures. Therefore, considerable investigations on InGaN QW structures were performed. Beside time-resolved and time-integrated luminescence spectroscopy, site-selective excitation spectroscopy as well as gain measurements were implemented.

An evidence of the presence of exciton localization was given by the characteristic temperature-dependence of the time-integrated luminescence recorded at low excitation densities [25]. In Figure 4 the evolution of the PL peak position and the full widths at half of maximum (FWHM) of the emission band are shown as a function of the temperature. The GaN luminescence (not shown here) in sample B fol-

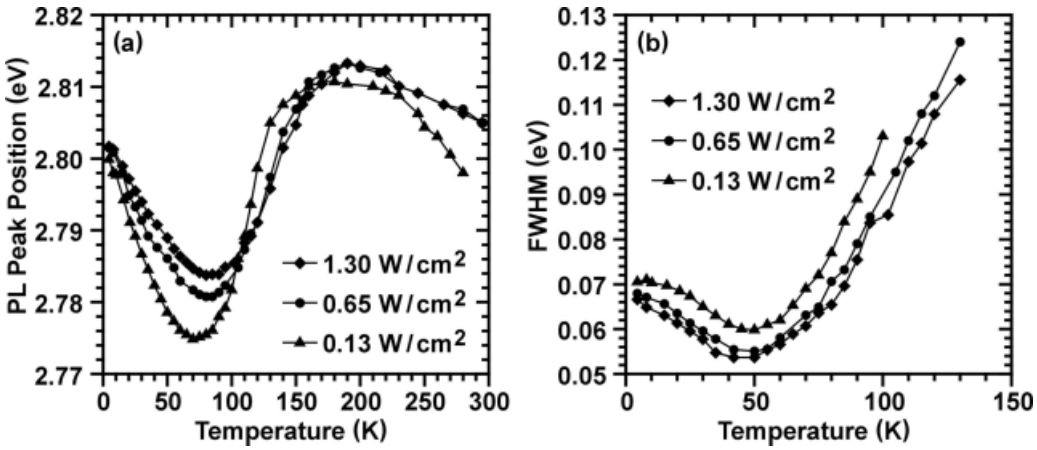

Fig. 4 Temperature dependence of PL peak position (a) and full width at half maximum (FWHM, b) of sample B for different PL excitation power. The increase of peak position energy above 70 K is caused by a carrier freeze out process.

lows Varshni's temperature dependence [26]. In contrast to the luminescence of GaN a strong S-shape behavior is observed for the InGaN-luminescence. Starting at 4.5 K for a PL excitation of 0.13 W/cm^2 an initial red shift of 25 meV leading to a minimum of the emission energy at 70 K. This red shift is compensated by a blue shift of 36 meV up to 170 K. For higher PL excitation densities the minimum becomes less pronounced and vanishes almost completely at an excitation power of 2.7 kW/cm². The thermal activation energies of 22 meV and 8 meV for the thermionic emission of the freezed out excitons were determined from an Arrhenius plot of the PL intensity. As it was theoretically shown by Zimmermann and Runge [27] the increase of the PL peak-position energy, namely the S-shape of the temperature dependence is caused by exciton freeze out in a system with randomly distributed potential fluctuations. Further evidence is obtained by absorption and site-selective spectroscopy.

A direct observation of the mobility edge (ME) is enabled by the site-selective spectroscopy. Here, the excitation energy is varied and the PL spectra are detected. In Figure 5 the energy of the PL maximum as a function of the excitation wavelength is depicted. Below a certain wavelength (above a certain energy given by the ME) no change of the PL maximum energy was detected. A further decrease of the excitation energy results in a significant shift of the PL maximum to lower energies. The shift rises linearly

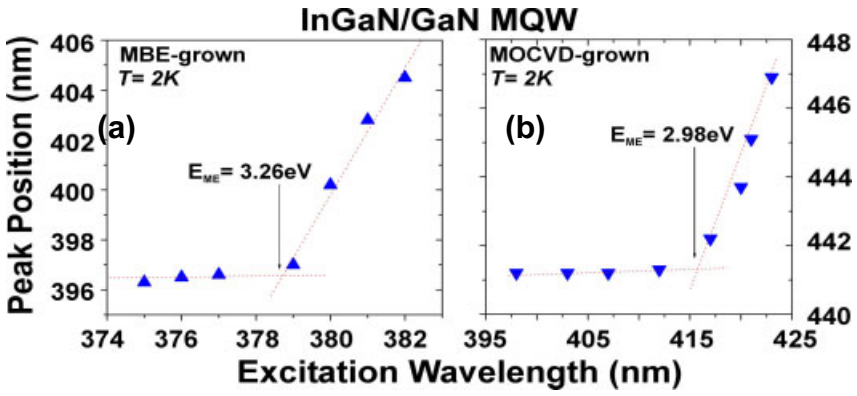

Fig. 5 (online colour at: www.interscience.wiley.com) Photoluminescence-maximum energy as a function of the excitation wavelength for two InGaN/GaN MQW samples (sample A, (a), and sample B, (b)). The excitation wavelength was varied below and above the mobility edge (ME). The ME (marked by arrows) was determined by extrapolation.

with decreasing excitation energy. Below a certain energy (marked by arrows in Figure 5), only the excitation of certain localized states are enabled. If the excitons are localized and there are no non-radiative centers within the localization length, there are two possibilities of relaxation: radiative decay or tunneling to localized states with lower energies. The latter is proportional to the number of states with lower energies and the excess energy (difference between the excitation energy and the energy of the localized states). Hence, an enhanced PL intensity of these localized states and a red shift of the PL maximum are observed. The values of the ME are determined by the linear extrapolation of the energy shift and the PL maximum for excitation above the localized states. They are in good agreement with the values obtained from absorption experiments. The presented results indicate exciton localization in QD-like structures at low excitation densities.

Beyond it, the processes determining the emission, optical gain and lasing at elevated excitation densities are to reveal. Especially, the influence of the exciton localization in QDs on the optical amplification is of a special interest. Therefore, the PL was analyzed up to excitation densities of several 100 $kWcm^{-2}$. In Figure 6 the PL-maximum energy as a function of the excitation density is shown for an InGaN/GaN MQW sample. A total blue shift with increasing excitation density of 190 meV was detected. The excitation density was varied by seven orders of magnitude. The linear dependence in the semi-logarithmic plot proves that the blue shift results from the successive filling of localized states (band-filling effect). Qualitatively it can be described by a Boltzmann distribution of the occupied states and an exponential DOS for excitons. In contrast, a nearly quadratic shift of the PL- maximum would result for piezoelectric fields. Following the estimation of the electric fields after Fiorentini et al. [12], a field of ~1 $MVcm^{-1}$ was obtained for the investigated MQW structure. An excitation density of 10 to 20 $kWcm^{-2}$ per well is necessary to screen these fields, what is close to the gain threshold density of the MOCVD-grown MQW structure (see also Fig. 8). Although this value is in reasonable agreement with the threshold density for the QCSE, no saturation at elevated excitation densities [12] and no typical nearly quadratic shift of the PL maximum were observed. As it was shown by Miller et al. [28] there are two major effects of an electric field applied perpendicular to the well on confined excitons. First, the exciton energy is reduced due to the bending of the confinement potential. The spatial separation of electron and hole wavefunction increases leading to a rising dipole character of the exciton. This effect leads to a red shift rising quadratically with electric field. Second, decrease of exciton binding energy due to reduced overlap of the wavefunctions. The latter effect amounts to ~10 % of the first and has an opposite sign. Thus, it can be concluded that at least at low temperatures the influence of internal fields in InGaN MQW structures is negligible in comparison to the localization of excitons in nm-scaled islands (QD-like structures).

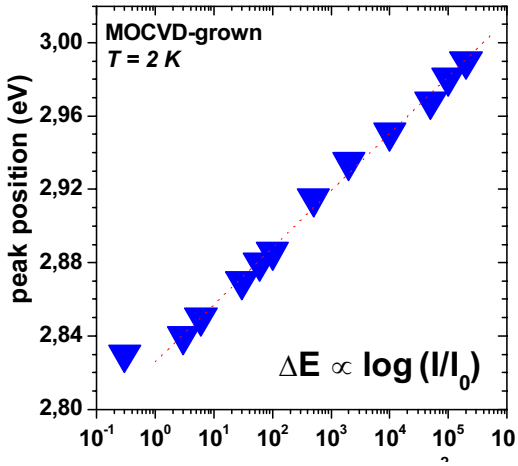

Fig. 6 (online colour at: www.interscience.wiley.com) Semi-logarithmic plot of the photoluminescence (PL)-maximum energy as a function of the excitation density for an InGaN/GaN MQW (sample B). The PL was detected at 6 K.

The results of excitation-density dependent PL are confirmed by time-resolved cathodoluminescence investigations. Here, the peak position of the emission line was detected as a function of the delay time and the excitation density. For the temporal shift of the InGaN peak a function $E_{Peak} = E_0 \pm 25$ meV log (t/t_0) is found (see Fig. 7a). This interpretation as a thermalization process within a statistical distribution of local energy states is strongly supported by excitation dependent cw measurements. Again, a monotonous blue shift of the main emission line according to $E_{Peak} = E_0 + 25$ meV log (P/P_0) is observed (Fig. 7b), directly visualizing the filling of the localized states.

The contribution of localized states to the gain and the lasing processes is revealed in Fig. 8. There, the low-excitation-density PL, the stimulated emission and the gain spectra for two different InGaN/GaN MQW samples are shown. The energy of the mobility edge is marked, too. Again a strong blue shift is observed for the PL maximum of the stimulated emission at elevated excitation densities. Lasing is detected in both samples at low temperatures. The threshold densities are given in Fig. 8. The onset of the lasing was observed at 3.0 eV for 160 kWcm^{-2} and at 3.22 eV for 1.2 MW cm^{-2}, respectively. With increasing excitation density a super linearly growth, line-shape narrowing and the characteristic polarization of the emission were observed. The maximum of the optical gain is blue shifted in comparison to the maximum of the stimulated emission. The energy of the ME is in the energy range of the gain. Thus, the contribution of localized states to the lasing processes is demonstrated. Nevertheless, gain and lasing are generated by de-localized carriers via band-band transitions, too. At room temperature (RT, not shown here) lasing is detected in the MOCVD-grown sample only. The lasing threshold is increased by a factor of four. The blue shift of the stimulated emission (in comparison to the low-excitation-density PL) is decreased, but ranges still between 50 to 100 meV. Because of the large localization energies (100 to 150 meV, note that the k_BT is 24 meV at RT) there is still a contribution of localized states to the emission processes.

Nevertheless, energy-selective spectroscopy did not reveal a shift of the PL maximum. Obviously, the ME behavior is not present at RT and the emission is dominated by de-localized transitions (band-to-band). This can be attributed to the effective temperature of an electron-hole plasma being by far higher than the lattice temperature. Therefore, the most localized states are depopulated by thermionic emission. In that case, the influence of the internal electric field may become more significant. The observed blue shift of the lasing energy with increasing excitation density at RT can be explained by the superposition of the band-filling processes of the remained localization sites and the screening of the electric fields. The lasing threshold matches to the value per QW predicted by Fiorentini et al. [12]. Again, the reduction of the emission efficiency due to the QCSE is shown.

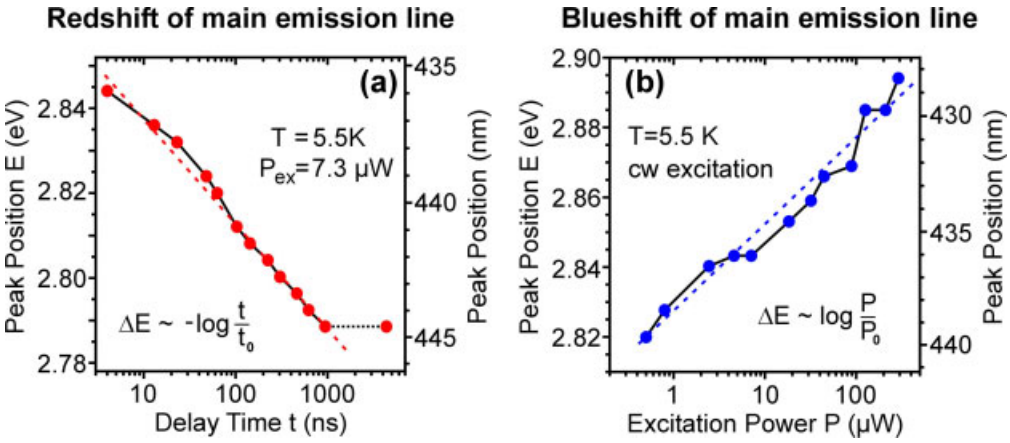

Fig. 7 (online colour at: www.interscience.wiley.com) a) Temporal red shift of the InGaN main emission line (sample B) due to exciton thermalization during decay and b) blue shift of InGaN main emission line (sample B) due to filling of localized states with increasing CL excitation power.

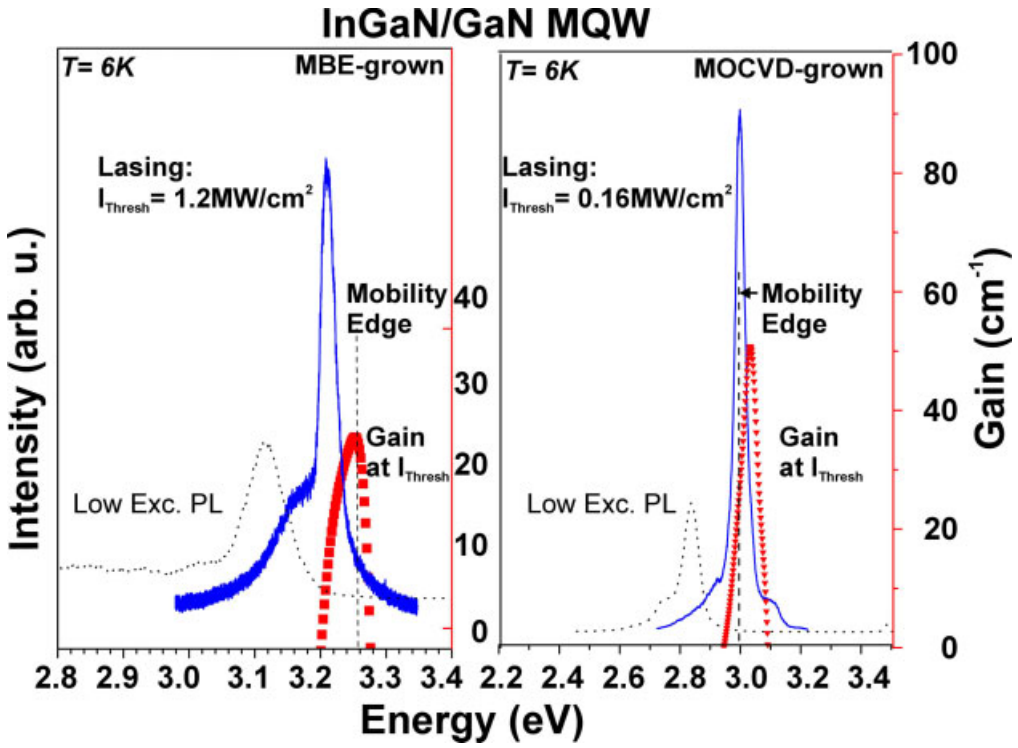

Fig. 8 (online colour at: www.interscience.wiley.com) Low-excitation-density PL (dotted lines), stimulated emission (straight lines) and gain spectra (symbols) for two different InGaN/GaN MQW samples. The energy of the mobility edge is marked by vertical dashed lines.

4 Conclusion

In principle two different localization mechanisms of charge carriers and excitons in ternary group-III nitride structures co-exist: first, the separate localization of electron and holes at the opposite interfaces of the quantum wells (QWs), described by the quantum-confined Stark effect (QCSE), and second, the localization of the free excitons in nm-scaled islands of local energy minima. Both effects superimpose and strongly affect the luminescence properties. The QCSE lead to a drop of the emission efficiency due to the reduction of the overlap of the carrier wavefunctions and the weakening of the excitons. This effect is caused by internal electric fields resulting from both, spontaneous polarization and piezo effect. It is always present in the nitrides. The second localization mechanism results from the spatial inhomogeneity due to nanoscopic fluctuations of the local composition. The strong spatial localization of excitons in nm-scaled islands of minimum energy dramatically improves the luminescence efficiency. The thermalization within the statistical energy distribution and the freeze out of the excitons in local minima at very low temperatures is directly proven by the characteristic S-shape temperature dependence of both, the luminescence peak energy as well as the full width at half of maximum (FWHM) of the luminescence line. Further evidence is given by the presence of a mobility edge for excitons. In particular for ternary QWs like InGaN/GaN the localization in nm-scale islands may completely determine the luminescence properties and dominate the QCSE.

Acknowledgements The authors thank the groups of H. Riechert (Infeneon), M. Heuken (Aixtron AG, Germany), H. Amano and I. Akasaki (Meijo University, Nagoya, Japan), for supplying the excellent samples. The authors gratefully acknowledge financial support by the Deutsche Forschungsgemeinschaft (DFG) in the framework of contracts Nos. Ho 1366/11-1, Ho 1366/11-2, CH 87/4-1, and CH 87/4-2.

References

[1] e.g., S. Chichibu, T. Azuhata, T. Sota, S. Nakamura, Appl. Phys. Lett. **69**, 4188 (1996).
[2] e.g., T. Takeuchi, S. Sota, M. Katsuragawa, M, Komori, H. Takeuchi, H. Amano, and I. Akasaki, Jpn. J. Appl. Phys. **36**, L382 (1997).
[3] e.g., M. Sugawara, Jpn. J. Appl. Phys. **35**, 124 (1996); K.P. O'Donnell, R.W. Martin, P.G. Middleton, Phys. Rev. Lett. **82**, 237 (1999); I.L. Krestnikov, N.N. Ledentsov, A. Hoffmann, D. Bimberg, A.V. Sakharov, W.V. Lundin, A.F. Tsatsul'nikov, A.S. Usikov, Zh.I. Alferov, Yu.G. Musikhin, D. Gerthsen, Phys. Rev. B **66**, 155310 (2002) and references therin.
[4] T. Riemann, D, Rudloff, J. Christen, A. Krost, M. Lünenburger, H. Protzmann, M. Heuken, phys. stat. sol. (b) **216**, 301 (1999).
[5] K.L. Shaklee, R.E. Nahory, and R.F. Leheny, J.Lumin. **7**, 284 (1973).
[6] J. Christen, *Advances in Solid State Physics* **XXXIII**, (Vieweg, Braunschweig, 1990, ed. U. Roessler), p. 239, (1990).
[7] J. Christen, T. Riemann, phys. stat. sol. (b) **228**, 419 (2001).
[8] e.g., F. Bernardini, V. Fiorentini, phys. stat. sol. (b) **216**, 391 (1999).
[9] e.g., T. Takeuchi, S. Sota, M. Katsuragawa, M, Komori, H. Takeuchi, H. Amano, and I. Akasaki, Jpn. J. Appl. Phys. **36**, L382 (1997).
[10] e.g., A. Hangleiter, J. Im, H. Kollmer, S. Heppel, J. Off, F. Scholz, MRS Internet J. Nitride Semiconductor Research **3**, 15 (1998).
[11] T. Takeuchi, S. Sota, M. Katsuragawa, M, Komori, H. Takeuchi, H. Amano, and I. Akasaki, Jpn. J. Appl. Phys. **36**, L382 (1997).
[12] V. Fiorentini, F. Bernardini, F. della Sala, A. di Carlo, P. Lugli, Phys. Rev. B **60**, 8849 (1999).
[13] H. Morkoc, *Nitride Semiconductors and Device* (Springer-Verlag, Berlin, 1999) and references therein.
[14] M. Leroux, N. Grandjean, M. Laugt, J. Massies, B. Gil, P. Lefebvre, P. Bigenwald, Phys. Rev. B **58**, R13371 (1998).
[15] G. Treatta, R. Cingolani, A. di Carlo, F. della Sala, P. Lugli, Appl. Phys. Lett. **76**, 1042 (2000).
[16] e.g., B. Gil, P. Lefebvre, J. Allegre, H. Mathieu, N. Grandjean, M. Leroux, J. Massies, P. Bigenwald, P. Christol, Phys. Rev. B **59**, 10246 (1999).
[17] A.Rizzi; R. Lantier, F. Monti, H. Lüth, F. della Sala, A. di Carlo, P. Lugli, J. Vac. Sci. Technol. B **17**, 1674 (1999).
[18] A. R. Smith, R. M. Feenstra, D. W. Greve, M.-S. Shin, M. Skowronski, J. Neugebauer, and J. E. Northrup, Appl. Phys. Lett. **72**, 2114 (1998).
[19] for a review see: I.L. Krestnikov, N.N. Ledentsov, A. Hoffmann, D. Bimberg, phys. stat. sol. (a) **183**, 207 (2001).
[20] e.g., S. Nakamura, Science **281**, 956 (1998).
[21] N.N. Ledentsov, Zh.I. Alferov, I.L. Krestnikov, W.V. Lundin, A.V. Sakharov, I.P. Soshnikov, A.F. Tsatsul'nikov, D. Bimberg, and A. Hoffmann, Comp. Semicond. **5** (**9**), 61 (1999).
[22] A.V. Sakharov, W.V. Lundin, I.L. Krestnikov,, V.A. Semenov, A.S. Usikov, A.F. Tsatsul'nikov, Yu.G. Musikhin, M.V. Baidakova, Zh.I. Alferov, N.N. Ledentsov, J. Holst, A. Hoffmann, D. Bimberg, I.P. Soshnikov, and D. Gerthsen, phys. stat. sol. (b) **216**, 435 (1999).
[23] e.g., Yu.G. Musikhin, D. Gerthsen, D.A. Bedarev, N.A. Bert, W.V. Lundin, A.F. Tsatsul'nikov, A.V. Sakharov, A.S. Usikov, I.L. Krestnikov, N.N. Ledentsov, A. Hoffmann, D. Bimberg, Appl. Phys. Lett. **80**, 2099 (2002).
[24] T. Degushi, A. Shikanai, T. Sota, S. Chichibu, S. Nakamura, Proc. ICNS'97, Tokushima; Japan, ed. K. Hiramatsu, 466 (1997).
[25] e.g., J. Holst, A. Kaschner, U. Gfug, A. Hoffmann, C. Thomsen, F. Bertram, T. Riemann, D. Rudloff, P. Fischer, J. Christen, R. Averbeck, H. Riechert, M. Heuken, M. Schwambera, O. Schön, phys. stat. sol. (a) **180**, 327 (2000) and references therein.
[26] Y.P. Varshni, Physica (Netherlands) **34**, 149 (1967).
[27] E. Runge and R. Zimmermann, Adv. Solid State Phys. **38**, 251 Σ1998); Phys. Status Solidi (a) **164**, 511 (1997).
[28] D.A.B. Miller, D.S. Chemal, D.C. Damen, A.C: Gossard, W. Wiegmann, T.H. Wood, C.A. Burrus, Phys. Rev. Lett. **53**, 2173 (1984).; D.A.B. Miller, D.S. Chemal, D.C. Damen, A.C: Gossard, W. Wiegmann, T.H. Wood, C.A. Burrus, Phys. Rev. B. **32**, 1043 (1985).